




Alkyl phosphate modified graphene oxide as friction and wear reduction additives in oil

Lei Zhang^{1,2}, Yi He^{1,3,*} , Lin Zhu^{1,*}, Zhilin Jiao⁴, Weizhou Deng⁴, Caiping Pu⁴, Chunmei Han⁴, and Shan Tang⁴

¹ College of Chemistry and Chemical Engineering, Southwest Petroleum University, Chengdu 610500, Sichuan, People's Republic of China

² Civil Aviation Flight University of China, Deyang 618300, Sichuan, People's Republic of China

³ Chengdu Evermaterials Co., Ltd, Chengdu 611730, Sichuan, People's Republic of China

⁴ PetroChina Chengdu Lubricant Company, Chengdu 610036, Sichuan, People's Republic of China

Received: 17 September 2018

Accepted: 30 November 2018

Published online:

5 December 2018

© Springer Science+Business Media, LLC, part of Springer Nature 2018

ABSTRACT

Alkyl phosphate modified graphene oxide (GON-DDP) was successfully synthesized using dodecanol, ethanol amine and self-made graphene oxide (GO) as precursors. The structure and morphology of GON-DDP were characterized by FT-IR, XPS, TG/DSC, SEM and TEM. The characterization results indicate that long alkyl phosphate chains were successfully grafted on GO surface, which guaranteed the dispersibility of GON-DDP in hydroisomerization dewax base oil (VHVI8). Then the tribology properties of GON-DDP as friction reduction and anti-wear additive in VHVI8 were evaluated on four-ball machine and SRV test system. The results show that the friction coefficient and wear scar diameter were reduced by 22.7% and 30.3% compared with bare VHVI8 base oil. Moreover, the non-seizure load of VHVI8 was significantly raised by adding GON-DDP. Finally, the lubrication mechanism was proposed according to Raman analysis on the worn surfaces of steel balls.

Introduction

Graphene was first prepared in 2004 and found to possess great talent in physical and chemical properties such as high mechanical strength, superconductivity, good transmittance, high thermal stability [1–5]. Thus, graphene and graphene derivatives have attracted extensive attractions in fundamental research such as structure, morphology features and intrinsic properties. In the recent few years, more and

more researches have been focusing on the technological development of macroscopic preparation, industrial production and potential application [6–11]. Furthermore, great technological breakthroughs have been made in many terminal application products.

As well known to us, friction and wear are the most important causes of energy consumption and materials losses [12, 13]. Choosing suitable additives is essential to formulate high performance lubricants.

Address correspondence to E-mail: chemheiyi@swpu.edu.cn; zhulinswpi65@gmail.com

Owing to the ultrathin lamellar structure, low shear stress, ultimate mechanical strength and high thermal stability, graphene and graphene derivatives possess potential application prospect as lubricant additive [14–18]. The challenge of graphene dispersion in oil has been solved in many research reports. Thus, many researchers have reported their work focusing on the lubricating properties of modified graphene. Khatri [19] have reported that octadecylamine-functionalized graphene oxide improves the performance of hexadecane by 26% and 9% reduction in friction coefficient and wear scar diameter, respectively. Cheng [20, 21] developed an oleic diethanolamide borate modified graphene oxide (ODAB) possessing good dispersibility and transparency in oil. Furthermore, the friction coefficient and wear scar diameter of base oil with 0.02 wt% ODAB were decreased by 38.4%, 42.0%, respectively. The maximum non-seizure load (P_B) increased by 46.2%. Also excellent friction reduction and anti-wear properties of alkylated graphene (AGN) have been verified in our previous work [22]. However, the anti-wear property of AGN under boundary was poor. According to the researches on the mechanism of many organic additives such as ZDDP and phosphonium alkyl phosphate ionic liquids [23, 24], we designed a new structure of alkyl phosphate modified graphene oxide (GON-DDP) to improve the boundary lubricating performance of modified graphene oxide [23, 25].

Boundary lubrication is very common among the four lubrication regimes, especially when the load is elevated. Boundary film always plays a very important role to protect the surfaces of friction pair when the oil film between moving solid surface breaks down. According to our previous research, alkylated graphene without active element or polar group possesses little boundary anti-wear property. Herein, we report the preparation of alkyl phosphate modified graphene oxide (GON-DDP) and the structure characterization by FT-IR, XPS, TG/DSC, SEM and TEM. The results show that the alkyl phosphate has been successfully grafted on GO surface by covalent bond. Then the tribological performances of VHVI8, which were evaluated using four-ball test machines and SRV test system, were significantly enhanced by adding a small quantity of GON-DDP, indicating its promising application potential as oil-based lubricant additive.

Experimental section

Materials

The graphene dioxide (GO) was prepared from natural graphite powder by the modified Hummer's method [26, 27]. The specific procedures have been reported in our previous work [28]. The hydroisomerization dewax base oil (VHVI8) was provided by PetroChina Lubricant Company, and its specifications are tabulated in Table 1. The other chemical reagents were analytical grade and purchased from Aladdin. All the materials mentioned above were used without any further purification.

Preparation and characterization of GON-DDP

As shown in Scheme 1, the phosphate ester modified graphene dioxide (GON-DDP) was prepared by two steps. All the reaction processes were conducted under the protection of nitrogen. The self-made GO was used as precursor after structure identification.

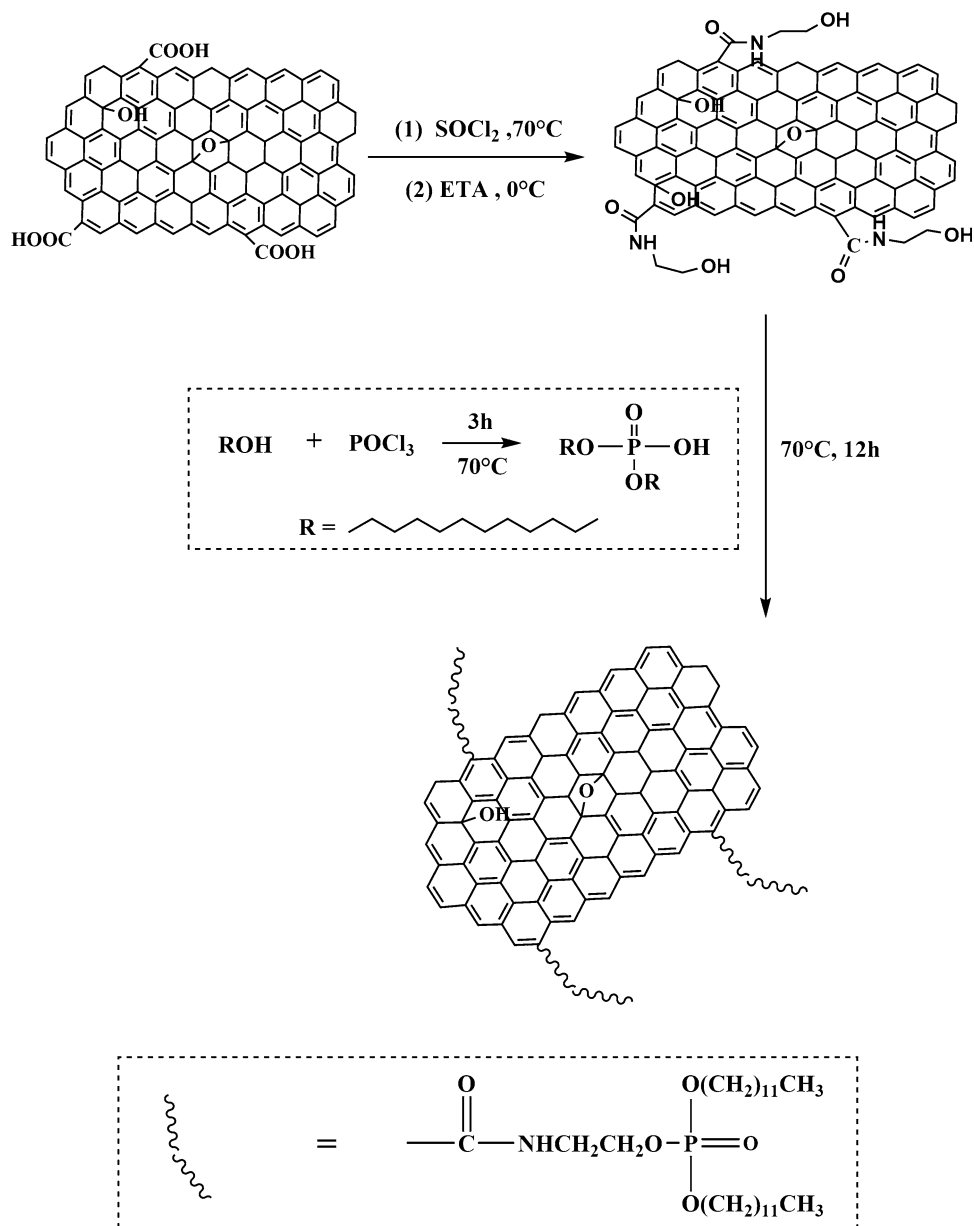
GO was first treated with SOCl_2 to activate the carboxylic groups. Briefly, 1 g GO and 20 mL SOCl_2 were mixed in a 250-mL flask, followed by 1-h reflux at 70 °C. The redundant SOCl_2 was distillation and recollected by heated the reaction system to 100 °C. Then the flask was transferred to an ice-water bath. The mixture of 5 mL ethanol amine (ETA) and 50 mL DMF was dropwise added and stirred for 1 h. The ETA modified graphene oxide (GON) was washed with ethyl alcohol and dried.

Then 0.06 mol phosphorus oxychloride was dropped into 0.12 mol liquid dodecanol and refluxed under the protection of nitrogen at 70 °C for about 3 h. Then 0.2 g GON was dispersed into the mixture by ultrasonic treatment. The mixture was treated under the protection of nitrogen while stirring at 70 °C for 12 h. Finally, the black powder (GON-DDP) was washed with ethyl alcohol and dried in oven at 60 °C. The structure of GO, GON and GON-DDP was characterized by FT-IR, XPS, TG/DSC, XRD and TEM.

Fourier transform infrared (FT-IR) spectra of GO, GON and GON-DDP samples were characterized on an infrared spectroscopy (FT-IR, WQF-520, Rayleigh) with KBr pellets as the sample matrix. The crystal structures were tested by X-ray diffraction (XRD) with Cu $K\alpha$ radiation source on a Thermo

Table 1 Physical and chemical properties of VHVI8 without and with GON-DDP (0.3 mg mL⁻¹) for tribology test

Sample ID	Density (20 °C) kg m ⁻³	Viscosity (40 °C), mm ² s ⁻¹	Viscosity (100 °C), mm ² s ⁻¹	Viscosity index	Pour point, °C
VHVI8	841.7	46.08	7.615	132	- 18
VHVI8 + GON- DDP	841.7	46.27	7.618	131	- 18

Scheme 1 Schematic mode for the fabrication of GON-DDP.

ESCALAB 250 instrument (PANalytical, Netherlands) with the 2θ angle ranges from 5° to 80° at a scan rate of 2°min^{-1} . Thermogravimetric analyses (TG/DSC) were carried out on a TG209F1 thermal

analyzer (Netzsch, Germany) with the temperature ranging from 50 to 900°C at a heating rate of $10^\circ\text{C min}^{-1}$. The morphology was observed by SEM

(FEI Magellan 400, USA, 5 kV) and TEM (JEM-2100, 200 kV) measurements.

Lubrication properties test

Different concentrations of GON-DDP dispersed in VHVI8 were blended by ultrasonic method. Then the tribological properties of VHVI8 with GON-DDP were evaluated in terms of frictional coefficient (COF) and wear scar diameter (WSD). The COF curves were measured on an SRV test system as per the standard ASTM D6425 (50 °C, 50 Hz, 200 N). Another types of COF of VHVI8 with different concentration of GON-DDP at varying load were tested on a four-ball test machine as per the standard ASTM D5183 (75 °C, 600 rpm), and the WSDs were tested on another four-ball machine as per the standard ASTM D4172 (75 °C, 1200 rpm, 392 N).

Results and discussion

Characterization of GON-DDP

FT-IR analysis

FT-IR analyses of intermediate and target products were carried out, and the results are shown in Fig. 1. The spectrum of GO presents the following characteristic peaks. The peaks at 1735 cm^{-1} in all spectra are assigned to the C=O on surface of GO and modified GO. The strong and broad bands of GO from around 3400 cm^{-1} are attributed to stretching vibration of O–H in –COOH. The same band in GON spectrum is attributed to O–H and N–H. However, the intensity of this broad band in GON-DDP has obviously declined, which is attributed to the converting of –COOH to –CONHC–. Simultaneously, there are new peaks in GON-DDP spectrum. The new strong peaks at 2922, 2850 and 1214 cm^{-1} are attributed to –CH₃, –CH₂– and P=O groups, respectively. According to the analysis of IR spectra, we can preliminary conclude that the alkyl phosphate long chains have been successfully grafted on GO surface.

XPS analysis

Figure 2 shows the XPS spectra of GO and GON-DDP. According to the C1s, spectrum of GO, C and O was detected in terms of peaks: C–C/C=C (284.8 eV),

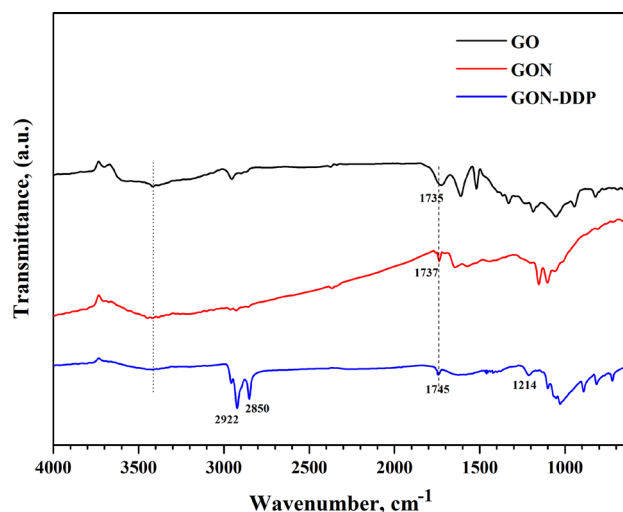


Figure 1 FTIR spectra of GO, GON and GON-DDP.

C–O (286.7 eV) and C=O (287.2 eV). In the spectra of GON-DDP (Fig. 2c), there were new signals of N and P detected in GON-DDP: C–N (400.6 eV) and P–O (134.2 eV). We can also observe that the intensity of C1s peak is higher than O1s in GON-DDP survey spectrum, which is opposite to that in the survey spectrum of GO. Moreover, the C/O atomic ratio of GON-DDP increased from 1.65 of GO to 3.83, indicating that long-chain alkyl has been introduced into the structure of GON-DDP. The conclusion above is consistent with that in FT-IR analysis.

XRD analysis

The XRD measurements were conducted to characterize the stacking state of GO and GON-DDP sheets. As shown in Fig. 3, the spectrum of GO shows identical diffraction peak of graphene oxide at $2\theta = 10.9^\circ$ [29]. However, the peak at $2\theta = 10.9^\circ$ disappeared in GON-DDP pattern. And there is a new weak and broad peak around $2\theta = 24.0^\circ$, indicating that the alkyl phosphate modified graphene oxide sheets are loosely stacked in GON-DDP powder. As shown in Scheme 1, the long alkyl chains were grafted on the surface of exfoliated GO sheets. With the intercalation of long alkyl group chains between the layers, the GON-DDP sheets are prevented from agglomerating. Therefore, they are loosely stacked and exist as an amorphous material instead of a lamellar crystal [30, 31].

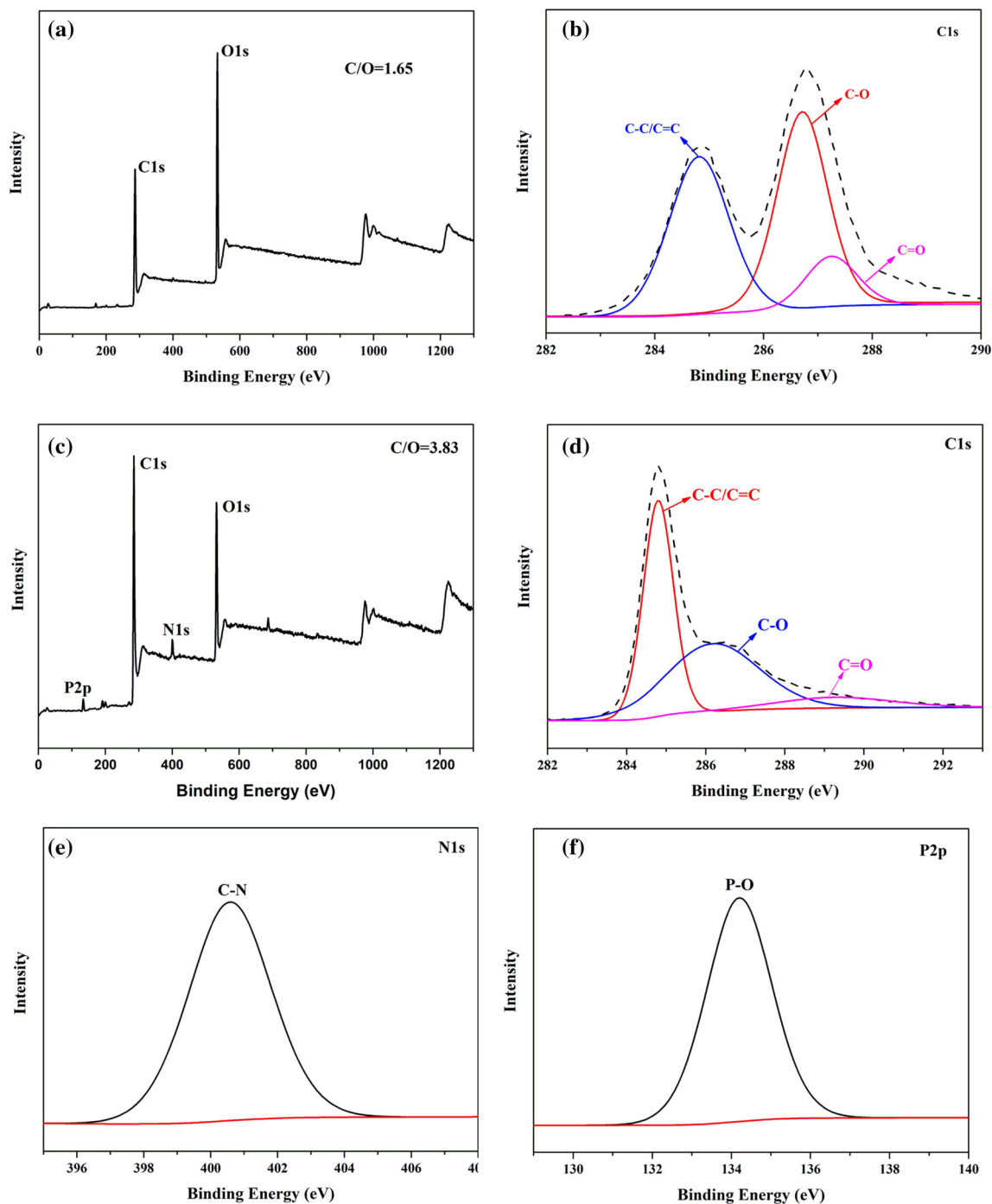


Figure 2 a XPS survey spectrum and b C1s spectrum of GO, c XPS survey spectrum, d C1s, e N1s and f P2p spectra of GON-DDP.

TG/DSC analysis

TG/DSC tests were carried out to evaluate the thermal decomposition properties of GO, GON and GON-DDP from 50 to 900 °C under flowing N₂. As shown in Fig. 4, GO suffers a small amount loss near 100 °C, which can be attributed to the loss of

adsorbed water in the samples. Subsequently, the major mass loss of GO around 220 °C can be accompanied by a vigorous release of gas, which is attributed to CO, CO₂ and steam release from labile functional groups [32, 33], resulting in a rapid thermal expansion of the powder material and large mass loss [34]. Similar analyses of self-made GO have been

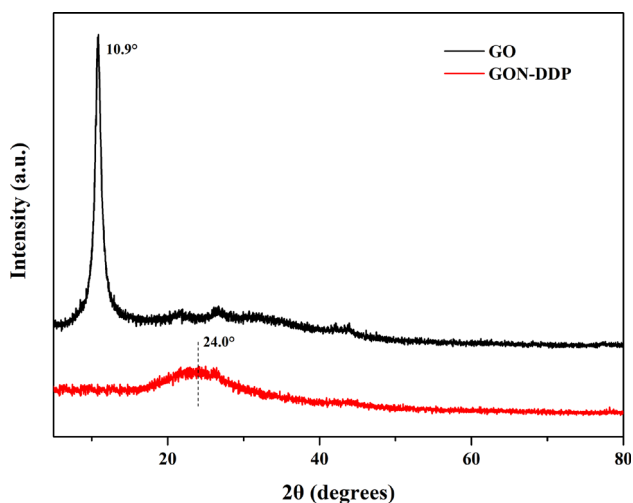


Figure 3 XRD patterns of GO and GON-DDP sheets.

proposed in our previous work [28]. As for GON, the mass loss was much less than GO, indicating that the thermal stability of GON was much better than that of GO. When comparing the weight loss and heat flow of GON and GON-DDP, we can find that even though the total weight loss of GON-DDP was about 20% less than that of GON (Fig. 4a), the heat flow of GON-DDP was always higher than GON (Fig. 4b). This phenomenon can be attributed to the higher thermal stability of GON-DDP sheets.

Morphology analysis of GON-DDP

The morphology investigations of GO and GON-DDP sheets were carried out on SEM and TEM instruments, and the results are shown in Fig. 5. The results

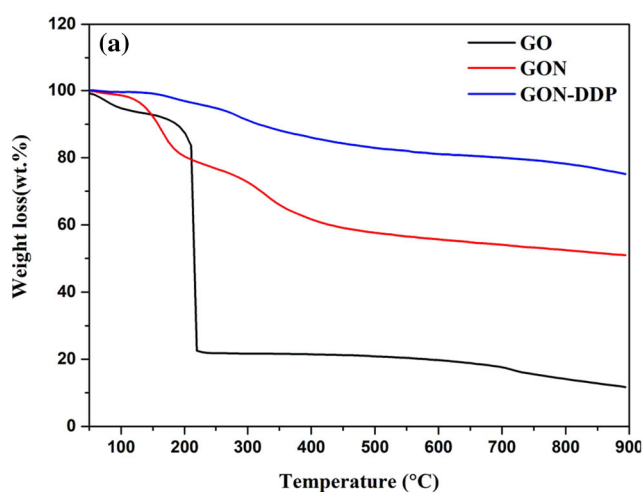


Figure 4 a TG and b DSC curves of GO, GON and GON-DDP.

shown in Fig. 5 clearly display the lamellar structure of GO and GON-DDP. Meanwhile, the wrinkles of sheets can be clearly observed in both GO and GON-DDP. Figure 5c presents the partial enlarged detail of Fig. 5b, showing the ultrathin structure and smooth surface of GON-DDP. This is essential to ensure the interposition of GON-DDP nanosheets into friction pairs.

Lubrication characterization of GON-DDP

Stable dispersibility in base oil is very important for GON-DDP as nano-lubricant. That is essential to guarantee the optimal lubricating property of GON-DDP sheets. Figure 6 shows different concentrations of GON-DDP sheets dispersed in VHVI8 base oil. GON-DDP sheets are nicely dispersed in base oil for 10 days. There is a little precipitation for 20-day settlement. The UV–vis absorbance spectra of VHVI8 base oil with GON-DDP are also displayed in Fig. 6. There is only a little reduction of the absorbance with longer time settlement, indicating that the GON-DDP sheets possess good dispersibility in VHVI8. This can be attributed to the van der Waals interaction between the grafted long alkyl chains on GON-DDP surface and hydrocarbon molecule of base oil.

The friction reduction and anti-wear properties were investigated using SRV system and four-ball test machine. First, the COF of GON-DDP in VHVI8 was tested on SRV test system in accordance with standard ASTM D6425 (50 °C, 50 Hz, 200 N). The results are shown in Fig. 7. The curves shown in Fig. 7a illustrate the fluctuation of COF. The initial

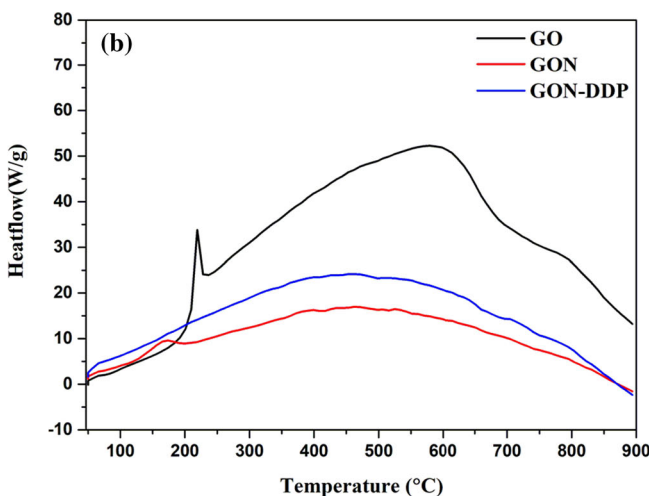


Figure 5 SEM images of **a** GO, **b** GON-DDP and **c** magnification of the highlight area in **(b)**. TEM images of **d** GON-DDP.

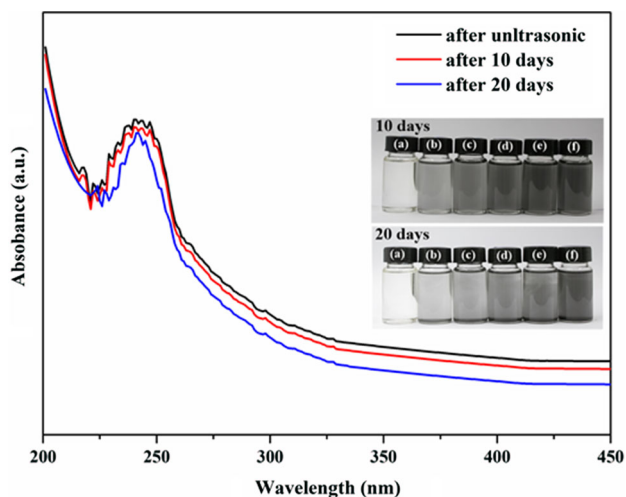
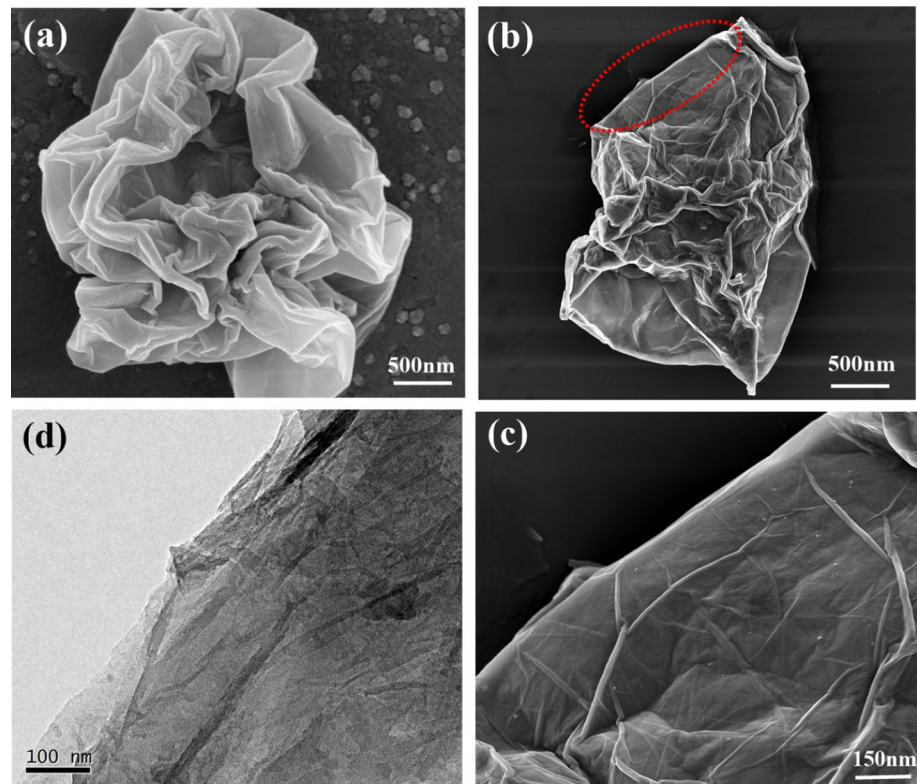


Figure 6 Digital images of VHVI8 base oil with different concentration of GON-DDP (**a–f** 0, 0.10, 0.20, 0.30, 0.40 and 0.50 mg mL⁻¹) settled for 10 days and 20 days. UV-vis absorption spectra of VHVI8 base oil containing GON-DDP (0.30 mg mL⁻¹) after ultrasonic treatment, 10-day and 20-day settlement.

high COFs around 0.13 at the beginning of friction test are attributed to the lack of lubricant between friction pairs. Subsequently, they all decline soon with the insertion of lubricant. As shown in Fig. 7a,

the COFs of bare base oil and low concentrate of GON-DDP (black and red curves) keep more stable than that of higher concentrate of GON-DDP (blue and purple curves) during early friction. However, this situation goes into reverse for longer friction especially after 2000s. The fluctuation range of black and red curves becomes larger than blue and purple ones, indicating that VHVI8 containing GON-DDP possesses more excellent lubricating property than bare VHVI8 after running-in. According to Fig. 7b, the average COF decreases with the concentration of GON-DDP increases. The lowest COF (~ 0.092) found at the concentration of 0.3 mg mL⁻¹ is reduced by 22.7% compared to pure VHVI8.

To investigate the boundary lubricating property of GON-DDP, a four-ball test was carried out in accordance with the standard ASTM D5183(75 °C, 600 rpm) and the results are shown in Fig. 8. Before the test was conducted, the steel balls must have passed the wear-in process using a standard wear-in lubricant, white oil having a viscosity at 40 °C of 24.3–26.1 cSt. Further test was carried out only when the wear-in scar diameter was 0.67 ± 0.03 mm (Fig. 8b). The test began with the load of 98 N. Then 98 N more load was added every 10 min until the friction trace indicated incipient seizure was

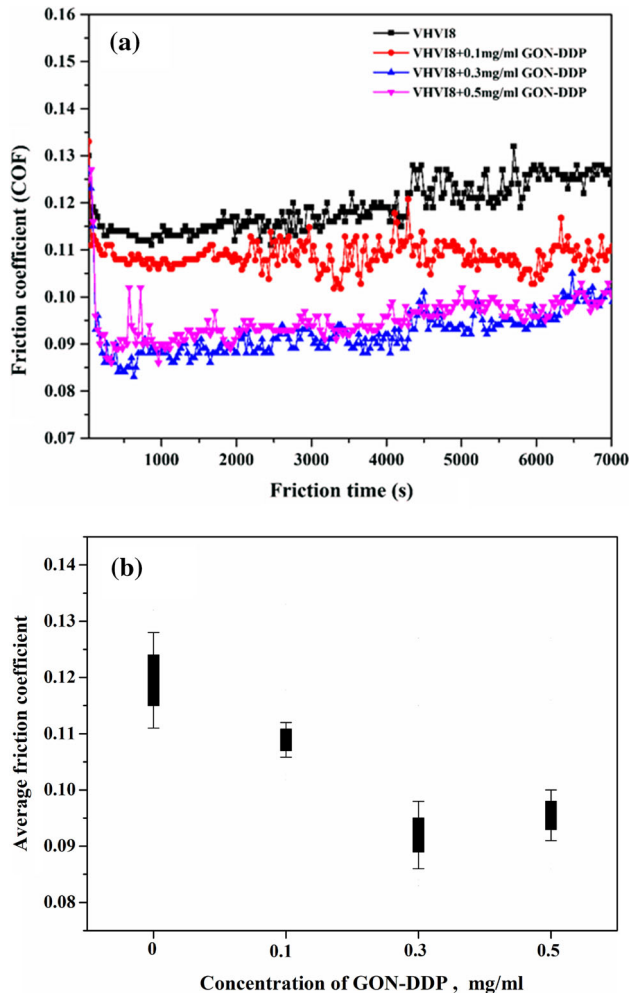


Figure 7 **a** Friction coefficient curves of VHVI8 with and without GON-DDP sheets and **b** average friction coefficient. Test condition: ASTM D6425, 50 °C, 50 Hz, 200 N.

occurring. The friction coefficient at the end of each 10-min interval was recorded, and the final wear scars on the three lower balls were measured.

As shown in Fig. 8a, the COF of all samples keeps rising with the increasing of load. It shows small differences between VHVI8 and the others in relatively low load area. Then the COF of VHVI8 base oil climbs sharply when the load reaches 294 N and then exceeds all other samples, indicating its weak boundary lubricating property. However, the COFs of VHVI8 containing 0.3 and 0.5 mg mL⁻¹ GON-DDP are lower and kept stable in high load area without no seizure occurring even when the load are 981 N. For the bare VHVI8 without and with 0.1 mg mL⁻¹ GON-DDP, the incipient seizure occurred at the load of 785 N, which is owing to the breakdown of boundary film. According to Fig. 8b, the oil with

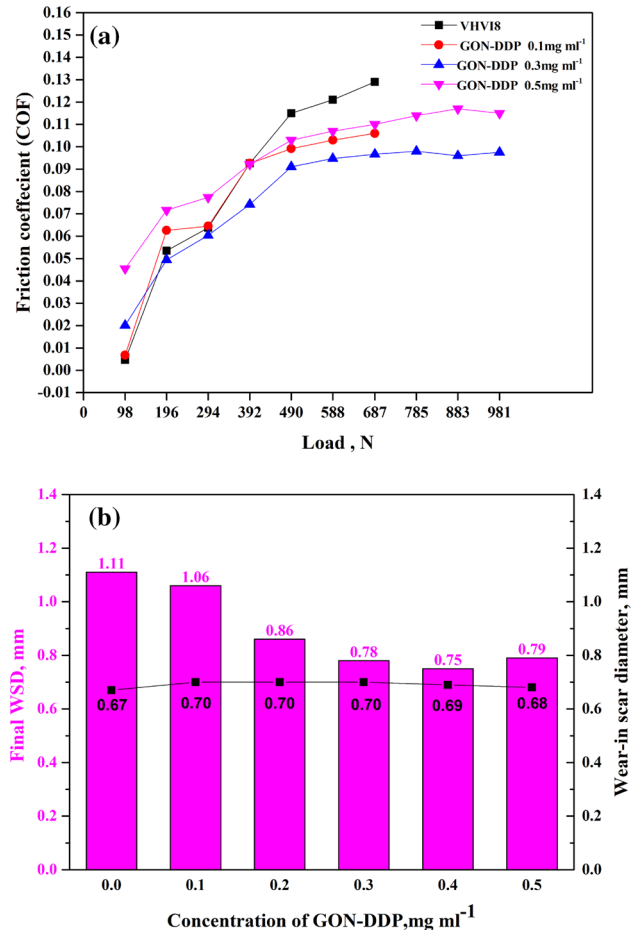


Figure 8 **a** Friction coefficient, **b** final wear scar diameter and wear-in scar diameter of VHVI8 with different concentration of GON-DDP at varying load. Test condition: ASTM D5183, 75 °C, 600 rpm.

higher concentration of GON-DDP shows much smaller final wear scar than bare base oil. In conclusion, the GON-DDP sheets significantly enhanced the friction reduction and boundary lubricating capability of VHVI8 base oil.

To acquire further understanding of anti-wear property of GON-DDP under boundary friction conditions, the tests as per ASTM D4172 (75 °C, 1200 rpm, 392 N, 60 min) were carried out. The results shown in Fig. 9 display that the WSD decreases with the increment of GON-DDP concentration to the lowest value 0.467 mm (about 30.3% decline compared to base oil). Then there is a slight increment as concentration of GON-DDP continues increasing. The SEM images of wear scar shown in Fig. 10 nicely confirm the results above. The comparison of wear scar in higher amplification (Fig. 10c, d) clearly displays the scratches. Obviously, the steel

ball lubricated by bare base oil VHVI8 shows much wider and deeper scratches than that lubricated by GON-DDP. This indicates that GON-DDP sheets can significantly enhance the anti-wear property of base oil.

Furthermore, to understand the role of GON-DDP in the lubrication process, Raman shift was detected on the worn surface of lower balls. As shown in Fig. 10e, there are two characteristic bands observed around 1300 cm^{-1} (D band) and 1570 cm^{-1} (G band) detected on the worn surface of steel ball that lubricated by GON-DDP. However, there is no Raman signal of graphene detected on the worn surfaces lubricated with bare VHVI8. The results above strongly indicate that the GON-DDP sheets have successfully entering the gap of friction pairs and deposited on the surfaces, forming excellent and essential boundary lubricating film on the steel balls. This confirms the previous speculations of lubrication mechanism of GON-DDP sheets.

Conclusions

In this report, the self-made GO has been modified with alkyl phosphate in two facile procedures to prepare a novel GON-DDP sheet. The followed characterization using FT-IR, XPS, TG/DSC, SEM and TEM confirms that the alkyl phosphate has been successfully grafted on GO surface, which guarantees the stable dispersibility of GON-DDP in VHVI8 base

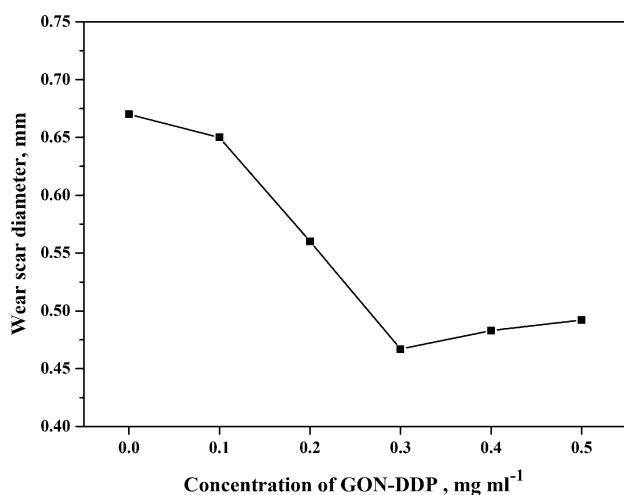


Figure 9 Wear scar diameter as a function of the concentration of GON-DDP sheets blended in VHVI8 base oil. Test condition: ASTM D4172, 75 °C, 1200 rpm, 392 N, 60 min.

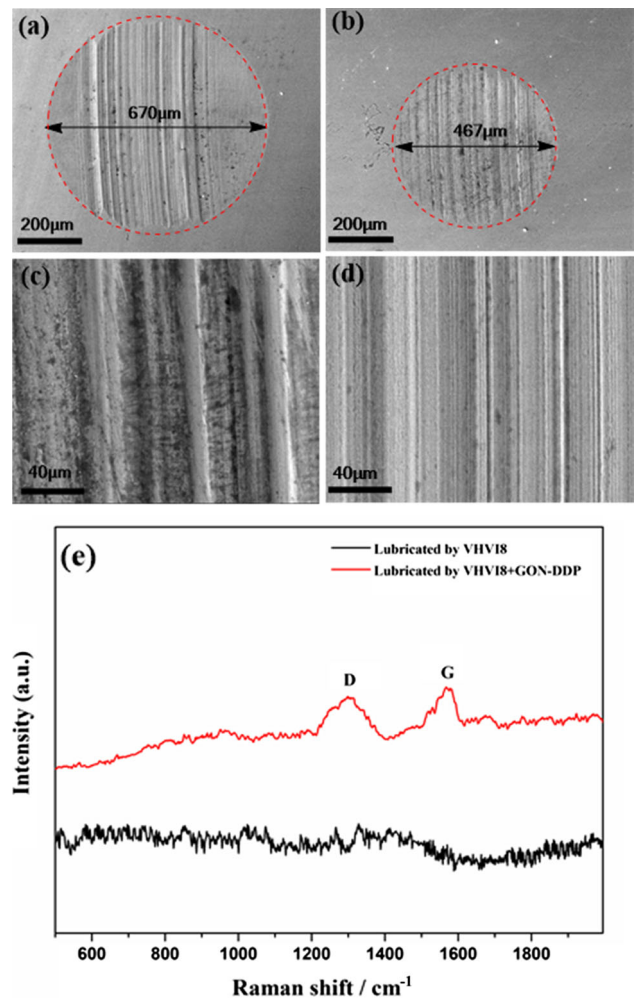


Figure 10 SEM images of the wear scar of steel balls lubricated by **a, c** bare VHVI8 and **b, d** VHVI8 containing 0.3 mg mL^{-1} GON-DDP sheets. **e** Raman shifts detected on the worn surfaces lubricated with and without GON-DDP sheets. Test condition: ASTM D4172, 75 °C, 1200 rpm, 392 N, 60 min.

oil. The results of tribological evaluations in terms of friction coefficient, wear scar diameter and incipient seizure load indicate that GON-DDP possesses promising application potential as friction reduction and anti-wear additive in VHVI base oil under boundary friction conditions.

Acknowledgements

This work was financially supported by National Natural Science Foundation of China (51774245) and Sichuan Province Applied Basic Research Project (2018JY0302).

References

- [1] Novoselov KS, Geim AK, Morozov SV, Jiang D, Zhang Y (2004) Electric field effect in atomically thin carbon films. *Science* 306:666. <https://doi.org/10.1126/science.1102896>
- [2] Stankovich S, Dikin DA, Dommett GH et al (2006) Graphene-based composite materials. *Nature* 442:282. <https://doi.org/10.1038/nature04969>
- [3] Wintterlin J, Bocquet ML (2009) Graphene on metal surfaces. *Surf Sci* 603:1841. <https://doi.org/10.1016/j.susc.2008.08.037>
- [4] Ramanathan T, Abdala AA, Stankovich S et al (2008) Functionalized graphene sheets for polymer nanocomposites. *Nat Nano* 3:327. <https://doi.org/10.1038/nnano.2008.96>
- [5] Park S, Ruoff RS (2009) Chemical methods for the production of graphenes. *Nat Nano* 4:217. <https://doi.org/10.1038/nnano.2009.58>
- [6] Zhang Y, Tan Y-W, Stormer HL, Kim P (2005) Experimental observation of the quantum Hall effect and Berry's phase in graphene. *Nature* 438:201. <https://doi.org/10.1038/nature04235>
- [7] Berger C, Song Z, Li T et al (2004) Ultrathin epitaxial graphite: 2D electron gas properties and a route toward graphene-based nanoelectronics. *J Phys Chem B* 108:19912. <https://doi.org/10.1021/jp040650f>
- [8] Eswaraiah V, Balasubramaniam K, Ramaprabhu S (2011) Functionalized graphene reinforced thermoplastic nanocomposites as strain sensors in structural health monitoring. *J Mater Chem* 21:12626. <https://doi.org/10.1039/C1JM12302E>
- [9] Gutierrez-Gonzalez CF, Smirnov A, Centeno A et al (2015) Wear behavior of graphene/alumina composite. *Ceram Int* 41:7434. <https://doi.org/10.1016/j.ceramint.2015.02.061>
- [10] Zhang L, Pu J, Wang L, Xue Q (2014) Frictional dependence of graphene and carbon nanotube in diamond-like carbon/ionic liquids hybrid films in vacuum. *Carbon* 80:734. <https://doi.org/10.1016/j.carbon.2014.09.022>
- [11] Eswaraiah V, Sankaranarayanan V, Ramaprabhu S (2011) Functionalized graphene–PVDF foam composites for EMI shielding. *Macromol Mater Eng* 296:894. <https://doi.org/10.1002/mame.201100035>
- [12] Holmberg K, Andersson P, Erdemir A (2012) Global energy consumption due to friction in passenger cars. *Tribol Int* 47:221. <https://doi.org/10.1016/j.triboint.2011.11.022>
- [13] Chu S, Majumdar A (2012) Opportunities and challenges for a sustainable energy future. *Nature* 488:294. <https://doi.org/10.1038/nature11475>
- [14] Berman D, Erdemir A, Sumant AV (2014) Graphene: a new emerging lubricant. *Mater Today* 17:31. <https://doi.org/10.1016/j.mattod.2013.12.003>
- [15] Wang X, Zhi L, Müllen K (2008) Transparent, conductive graphene electrodes for dye-sensitized solar cells. *Nano Lett* 8:323. <https://doi.org/10.1021/nl072838r>
- [16] Lee C, Wei X, Kysar JW, Hone J (2008) Measurement of the elastic properties and intrinsic strength of monolayer graphene. *Science* 321:385. <https://doi.org/10.1126/science.1157996>
- [17] Porwal H, Tatarko P, Saggarr R et al (2014) Tribological properties of silica–graphene nano-platelet composites. *Ceram Int* 40:12067. <https://doi.org/10.1016/j.ceramint.2014.04.046>
- [18] Lee C, Li Q, Kalb W et al (2010) Frictional characteristics of atomically thin sheets. *Science* 328:76. <https://doi.org/10.1126/science.1184167>
- [19] Choudhary S, Mungse HP, Khatri OP (2012) Dispersion of alkylated graphene in organic solvents and its potential for lubrication applications. *J Mater Chem* 22:21032. <https://doi.org/10.1039/c2jm34741e>
- [20] Zhi-Lin Cheng WL, Pei-Rong Wu, Liu Zan (2017) A strategy for preparing modified graphene oxide with good dispersibility and transparency in oil. *Ind Eng Chem Res* 56:5527–5534. <https://doi.org/10.1021/acs.iecr.7b01472>
- [21] Cheng Z-L, Li Y-X, Liu Z (2017) Novel adsorption materials based on graphene oxide/Beta zeolite composite materials and their adsorption performance for rhodamine B. *J Alloys Compd* 708:255. <https://doi.org/10.1016/j.jallcom.2017.03.004>
- [22] Zhang L, He Y, Zhu L, Yang C, Niu Q, An C (2017) In situ alkylated graphene as oil dispersible additive for friction and wear reduction. *Ind Eng Chem Res* 56:9029. <https://doi.org/10.1021/acs.iecr.7b01338>
- [23] Zhang J, Spikes H (2016) On the mechanism of ZDDP antiwear film formation. *Tribol Lett* 63:24. <https://doi.org/10.1007/s11249-016-0706-7>
- [24] Li H, Somers AE, Rutland MW, Howlett PC, Atkin R (2016) Combined nano- and macrotribology studies of titania lubrication using the oil-ionic liquid mixtures. *ACS Sustainable Chem. Eng.* 4:5005. <https://doi.org/10.1021/acssuschemeng.6b01383>
- [25] Qu J, Barnhill William C, Luo H et al (2015) Synergistic effects between phosphonium-alkylphosphate ionic liquids and zinc dialkyldithiophosphate (ZDDP) as lubricant additives. *Adv Mater* 27:4767. <https://doi.org/10.1002/adma.201502037>
- [26] William JBY, Hummers S, Offeman RE (1958) Preparation of graphitic oxide. *J Am Chem Soc* 80:1339
- [27] Mungse OPSHP, Sugimura H, Khatri OP (2014) Hydrothermal deoxygenation of graphene oxide in sub- and supercritical water. *RSC Adv* 4:22589. <https://doi.org/10.1039/C4RA01085J>

- [28] Zhang L, He Y, Feng S et al (2016) Preparation and tribological properties of novel boehmite/graphene oxide nanohybrid. *Ceram Int* 42:6178. <https://doi.org/10.1016/j.ceramint.2015.12.178>
- [29] Wang A, Li X, Zhao Y, Wu W, Chen J, Meng H (2014) Preparation and characterizations of Cu₂O/reduced graphene oxide nanocomposites with high photo-catalytic performances. *Powder Technol* 261:42. <https://doi.org/10.1016/j.powtec.2014.04.004>
- [30] Zhang K, Zhang LL, Zhao XS, Wu J (2010) Graphene/polyaniline nanofiber composites as supercapacitor electrodes. *Chem Mater* 22:1392. <https://doi.org/10.1021/cm902876u>
- [31] Park S, An J, Potts JR, Velamakanni A, Murali S, Ruoff RS (2011) Hydrazine-reduction of graphite-and graphene oxide. *Carbon* 49:3019. <https://doi.org/10.1016/j.carbon.2011.02.071>
- [32] Wang G, Yang Z, Li X, Li C (2005) Synthesis of poly(aniline-co-*o*-anisidine)-intercalated graphite oxide composite by delamination/reassembling method. *Carbon* 43:2564. <https://doi.org/10.1016/j.carbon.2005.05.008>
- [33] Lerf A, He H, Forster M, Klinowski J (1998) Structure of graphite oxide revisited. *J Phys Chem B* 102:4477. <https://doi.org/10.1021/jp9731821>
- [34] Stankovich S, Dikin DA, Piner RD et al (2007) Synthesis of graphene-based nanosheets via chemical reduction of exfoliated graphite oxide. *Carbon* 45:1558. <https://doi.org/10.1016/j.carbon.2007.02.034>